

Design and Analysis of a Novel-shaped Hexa-Band Frequency Reconfigurable antenna integrated with PIN diode for S-Band and 5G Sub-6 GHz Applications

Athira Mohan R K¹, K G Padmasine²

^{1,2} Department of Electronics and Instrumentation, Bharathiar University, Coimbatore

Abstract - The work presents a novel shaped hexa-band frequency reconfigurable antenna. Depending upon the switching states, it can take place with three Switching states. For the three switching, two single band modes (3.5 and 5.4 GHz) and two dual band modes (2.29, 4.21, 2.6 and 5.2 GHz). The desired operating characteristics were accomplished using a number of switching states. The intended antenna performs in a dual band mode when all of the switches are switched ON, and it operates in a single band mode when all of the switches are turned OFF. It functions in a dual band mode when two switches are in the ON position and one switch is in the OFF position. When both switches were OFF and one switch was ON, the antenna performed on a single resonant band. In the simulation platform, lumped constituents are used to generate tunable capacitance, which is liable for frequency reconfigurability. The fabricated antenna's evaluated tuning capability covers from 2.29 GHz to 5.2 GHz. For the different operating conditions of the described hexa-band antenna, remarkable efficiencies, suitable radiation patterns, appropriate gain, enhanced impedance matching, and directivity values were attained. Ansys HFSS is used to examine the far field and scattering properties. The developed antenna may very well be seamlessly implemented into modern communications systems due to its compact and inexpensive architecture. To evaluate the simulation results, a prototype of the proposed antenna is fabricated and analyzed using PIN diode switches. The measured and simulated findings for the proposed reconfigurable antenna are in excellent agreement.

Key Words: Frequency Reconfigurable, Reconfigurable Antenna, PIN Diode, Wireless Communication, 5G

1. INTRODUCTION

The requirement for portable electronic devices performing at numerous frequency ranges for various applications is growing as a result of the increasing innovation of electronics and wireless communication. Advanced communication technologies require multi-band and customizable antennas. Because of their usefulness in modern mobile communications services, Reconfigurable antennas have gained considerable attention. The attributes of reconfigurable antennas have been used to obtain selectivity in the polarization, pattern, and frequency of the radiating structure, enabling them to substitute multi-band typical antennas [1]. A cognitive radio design is the method of the future regarding wireless communication, and it necessitates a sensing antenna that can observe the spectrum and be tuned up to a specific frequency range. Satellite communications and multi-radio wireless applications require frequency reconfigurable antennas [2]. Because of its superiority in beam reconfigurability, pattern reconfigurable antennas are preferred for multiple input multiple output

(MIMO) operations. Based on the wireless channel, pattern reconfigurable antennas modify the radiation pattern to strengthen the antenna's directivity and gain in the preferred manner [3]. In a wireless communication technology, polarization reconfigurable antennas are often used to repurpose the frequency and minimize interference. The frequency reconfigurable antennas can tune to the antenna's frequency response according to the user's requirements. Various switching approaches that alter the current flow pattern in the radiation pattern can be used to achieve antenna reconfigurability. PIN diodes, micro-electromechanical switches, lumped components, optical switches, varactor diodes, and electronic radio frequency switching devices can all be implemented to accomplish the reconfigurability characteristic [4]. When contrast to PIN diodes, MEMS have number of desirable characteristics, including minimal insertion loss, effective isolation, minimum power handling, and low cost [5].

The research community has turned their attention on reconfigurable antennas because of its appealing features such as minimal cost, simple structure, maximum efficiency, ease of fabrication, simple integration, and Omni directional pattern. In [6], Two triple-band monopole antennas for handheld wireless applications including Wi-Fi, WiMAX, and WLAN are suggested in this paper. Using a FR4 material with a thickness of 1.6 mm, an efficient and advanced frequency reconfigurable monopole antenna has been designed in this article. The designed antenna can function for both single and dual band mode (WiMAX at 3.5 GHz, Wi-Fi at 2.45 GHz and WLAN at 5.2 GHz) [7]. Within the radiating element of the proposed antenna, lumped elements are used to achieve reconfiguration. This work [8] features a dual band monopole antenna that was initially designed for wireless purposes. The suggested antenna is made up of a rectangular patch monopole with a slot cut out for dual band operation and a smaller dimension. The antenna consists in the 2.3 to 3.4 GHz and 4.95 to 5.85 GHz frequency bands. In wireless communications, these bands are now extensively used. This compact dual band monopole antenna is a great option for wireless devices that need to communicate with the outside world.

The concept of a wearable dual band frequency reconfigurable microstrip patch antenna for wireless communication applications (i.e. Wi-Fi at 2.44 GHz and WiMAX at 3.54 GHz) is discussed in this study [9]. A reconfigurable antenna for quad-band mobile device applications is proposed in this communication [10]. When compared to existing passive quad-band antennas, the suggested antenna has a simple structure of bias network related to PIN diode. An F-shaped frequency reconfigurable antenna for GSM, Wi-Fi, WLAN, and WiMAX applications has been designed in this study [11].

Depending on the state of the switches being employed, the antenna can perform in several bands.

Here the antenna is a planar small quad band reconfigurable antenna for GNSS, lower WiMAX, WLAN, and X-band applications [12]. The antenna's frequency switching capabilities are implemented using a PIN diode. In terms of process ability, the switch improves efficiency than the antennas with a standard multiband configuration. A reconfigurable stubbed ground structure is also used to generate a frequency-reconfigurable coplanar-waveguide (CPW) fed monopole antenna [13]. The antenna can be reconfigured in three operating parameters: single-band, dual-band and triple-band using four PIN diodes in the stubs extending from the ground. Here [14] a circular slot ultra-wideband (UWB) antenna with dual band-notched multimode reconfigurable properties is proposed. Dual band notched function is achieved using a multiple T-shaped stepped impedance resonator (TS-TSIR) and a simultaneous stubs loaded resonator (PSLR) to deny global interoperability.

This study [15] provides a unique four-band frequency reconfigurable antenna for the GNSS (Global Navigation Satellite System), WiMAX (Lower Worldwide Interoperability for Microwave Access), WLAN (Wireless Local Area Network), and X-band. When compared to traditional multiband antennas, the antenna's frequency switching capabilities provided by a PIN diode switch improve efficiency in terms of process ability. On an FR-4 substrate, a compact unique shaped, hexa-band, and efficient frequency reconfigurable monopole antenna is designed in this research. WLAN, Wi-Fi, WiMAX, and UMTS are all covered by the monopole antenna. To achieve frequency reconfigurability in the simulation, the lumped element components (i.e., RLC; resistance, inductance, and capacitance) can be used as switches within the radiating structure of the developed antenna. Each switch has a 1 mm slot set aside for its implementation. PIN diodes, on the other hand, are implemented in the measurement to achieve frequency reconfigurability. The remaining part of the paper is arranged in the following pattern. The concept, design, and operating mechanisms of the innovative hexa-band antenna are covered. The simulated and measured environments, as well as the outcomes and the next design with simulated and measured results are given.

2. PARAMETRIC STUDY

The basic geometry, conceptual design, and switching mechanisms of the suggested hexa-band frequency reconfigurable monopole antenna are discussed and summarized in this section. The proposed antenna is altered in the simulation environment through lumped element switches to achieve two single band and two dual band modes. Furthermore, to achieve reconfigurability, PIN diodes are incorporated in the measuring setup. To enhance efficiency and achieve satisfactory far field radiation patterns, a shortened metallic ground plane is employed on the rear. Figure 1 illustrates the structural dimensions and layout of the designed hexa-band frequency reconfigurable antenna for UMTS, Wi-Fi, WiMAX, WLAN and 5G applications.

The proposed antenna's radiating element is printed on a lossy FR-4 substrate with a relative permittivity of 4.4 and a tangent loss of 0.02, which is supported by a truncated metallic ground

surface. Because the FR-4 substrate is widely available, the antenna design is more inexpensive and viable. The truncated metallic ground surface has the characteristic of providing the best gain, efficiency, and directivity. For antenna excitation, a 50 micro strip line with a width of 3 mm is employed. The antenna is excited using the waveguide port attached to the feed line. As demonstrated in Figure 1, four 1 mm wide slots in the radiating structure are designated for the implementation of lumped element switches. The suggested monopole antenna has a volume of $33 \times 16 \times 1.6 \text{ mm}^3$. Table 1 illustrates the proposed structure's specific dimensions.

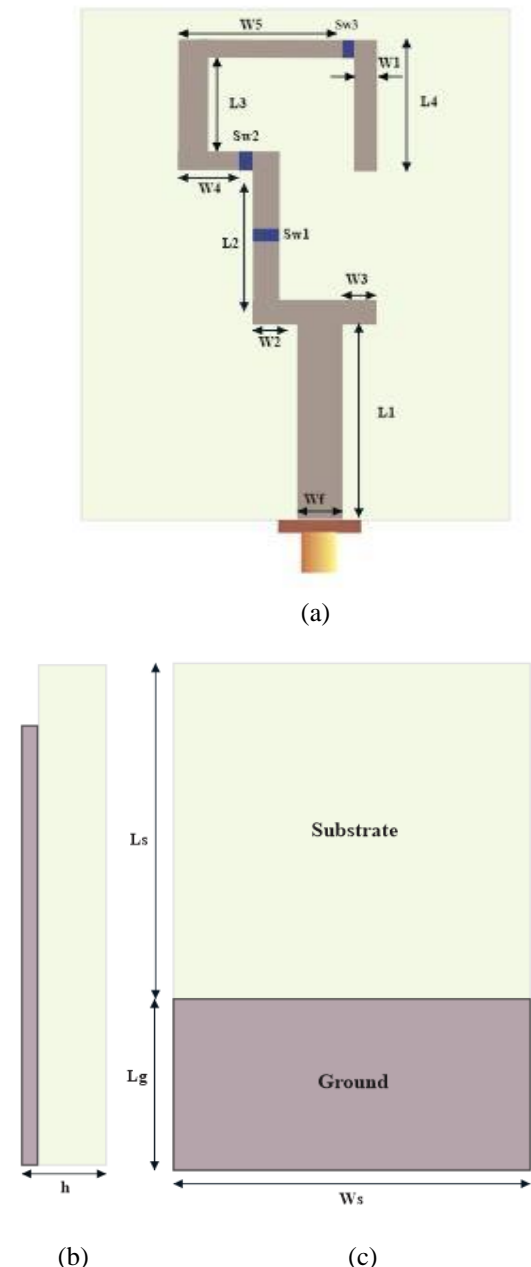


Figure 1. Layout of the designed Hexa-Band Frequency Reconfigurable Antenna with three PIN diodes: (a) Front view (b) Side view (c) Rear view.

Table 1. Dimensions of the Proposed Design

Sl.No	Dimensions	Values
1.	L_1	15
2.	L_2	9.1
3.	L_3	4.5
4.	L_F	6.8
5.	L_S	33
6.	L_G	7.5
7.	W_1	2
8.	W_2	2.5
9.	W_3	3
10.	W_4	2
11.	W_5	6.3
12.	W_F	3
13.	W_S	16
14.	H	1.6

2.1 Design Theory and Equations

For the interconnection of the switches within the proposed design, 1 mm slots in the radiating patch are designated. The transmission line model principle is used to evaluate the resonant lengths of the proposed antenna, which are $S_{2.29}$, $S_{2.6}$, $S_{3.5}$, $S_{4.21}$, $S_{5.2}$, and $S_{5.4}$. Changing the switching states results in the resonant frequencies modes. The directed wavelength and resonant lengths are referred to as:

$$S_{2.29} = \lambda_{2.29}/4 \quad (1)$$

$$S_{2.6} = \lambda_{2.6}/4 \quad (2)$$

$$S_{3.5} = \lambda_{3.5}/4 \quad (3)$$

$$S_{4.21} = \lambda_{4.21}/4 \quad (4)$$

$$S_{5.2} = \lambda_{5.2}/4 \quad (5)$$

$$S_{5.4} = \lambda_{5.4}/4 \quad (6)$$

The directed wavelength and antenna quality were also maximized for adequate radiation efficiency, which can be calculated using the equation. The surface current distribution for a particular frequency mode is being used to calculate the appropriate resonant length, which is expressed in terms of directed wavelengths, l_g , as given:

$$L_{fr} = \frac{\lambda_g}{4} = \frac{C}{4f_r\sqrt{\epsilon_e}} \quad (7)$$

where, C is the velocity of light and f_r is the resonance frequency and ϵ_e is the effective permittivity. The effective permittivity can be expressed as

$$\epsilon_e = \frac{\epsilon_r + 1}{2} + \frac{\epsilon_r - 1}{2} \left(1 + 12h/w\right)^{-0.5} \quad (8)$$

where, W is the width of radiating element of the antenna, h is the height of substrate, and ϵ_r is the relative permittivity. When the antenna is excited at the exact point, the efficiency

increases, resulting in a decrease in the reflection coefficient, which is described in a mathematical model as:

$$|\Gamma| = \frac{Z_a - Z_c}{Z_a + Z_c} \quad (9)$$

where, Z_a is the antenna impedance and Z_c is the characteristic impedance of the feed line. The reflection coefficient (S_{11}) and VSWR are multiple antenna parameters that are linked. The definition of VSWR is

$$VSWR = \frac{1 + |\Gamma|}{1 - |\Gamma|} \quad (10)$$

In the desired frequency range, the antenna has a relatively low reflection coefficient when exactly suited. The radiation efficiency associates the proposed antenna's directivity and gain. The gain is commonly expressed in decibels (dB) and is stated as follows:

$$G(dB) = 10 \log_{10}(\eta_{rad} D) \quad (11)$$

where, G is the gain and D is the directivity of the proposed antenna.

2.2 Switching Techniques

PIN diodes function as variable resistors at RF frequencies. PIN diodes, on the other side, have slightly more complicated circuitry for the ON and OFF states. In the equivalent circuit, PIN diodes have an inductance (L_b) in both ON and OFF states. The low resistance (R_{bs}) was included in the ON state which is forward biased, while the equivalent PIN was included in the OFF state and is reverse biased. As shown in Figure, a diode circuit is made up of a parallel combination of resistance (R_{bp}) and capacitance (C_c). As possible, the PIN diodes are structured as two lumped RLC boundary conditions, as shown in the Figure 2. The suggested antenna's reconfigurable features have been designed to simulate only by using resistors. Users did not consider capacitance and inductance values in the simulation because the switch is on the ON-state in both the RLC lumped model and the PIN diode model provides a short circuit characteristic, enabling current to flow along the structure's radiating path. In the OFF state, however, both models exhibit an open circuit phenomenon, impeding the flow of current. The equivalent circuit model for both the ON and OFF states of the PIN diode model has already been discussed. According to the research, the ON state in the PIN diode model is recognized as a series RL component with small values that performs as a short circuit, allowing current to flow along the radiator. In contrast to this, the OFF state of a PIN diode is simulated as a parallel RLC component with such values that it demonstrates an open circuit behavior in which current cannot flow along the radiator. To simplify our model, designers focused on open circuit and short circuit actions, and the switch was discovered as an RLC lumped element model with only resistor values. A resistor R_{bs} with a limited value of 1 ohm acts as a short circuit and enables normal current flow. A resistance R_{bp} of 1 Mega ohm, on the other hand, demonstrates open circuit behavior and stops the path for current to flow along the radiating structure.

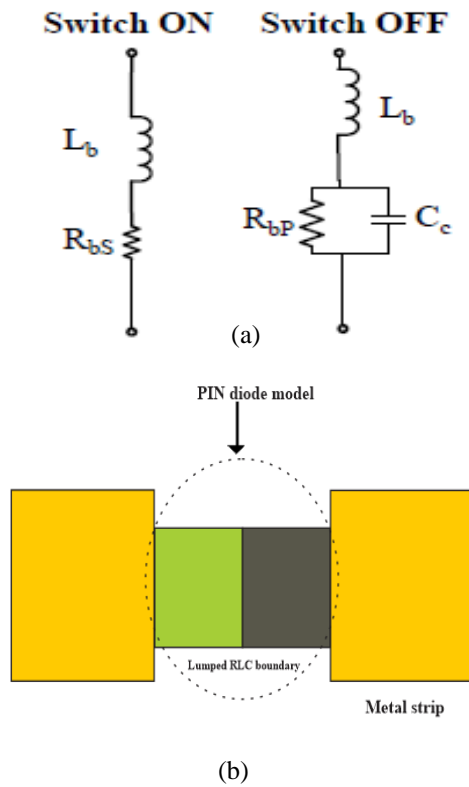


Figure 2. RF PIN Diode Configuration (a) Equivalent circuit models for the ON and OFF states of the switch (b) PIN Diode model.

2.3 Simulated and Measured Results

The radiating structure is designed, modelled, and examined using Ansys HFSS to investigate the performance of the hexa-band antenna. A waveguide port is often used as an excitation source for the proposed antennas. The VSWR, gain, directivity, far field pattern, reflection coefficient, and surface electric-field are measured in Ansys HFSS using the transient solver with open-add-space boundary conditions.

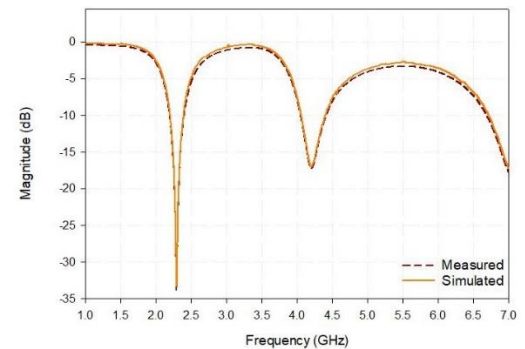
Table 2. Tuning states of the Hexa-band frequency antenna

Sl.No	SW1	SW2	SW3	Frequency States
1.	ON	ON	ON	Dual band (2.29 GHz and 4.21 GHz)
2.	ON	ON	OFF	Dual band (2.6 GHz and 5.2 GHz)
3.	ON	OFF	OFF	Single band (3.5 GHz)
4.	OFF	OFF	OFF	Single band (5.4 GHz)

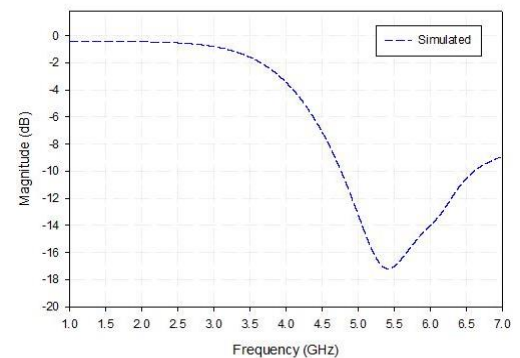
The proposed antenna operates in a dual band frequency mode with a return loss of -32.9435 and -17.2412 dB at 2.29 and 4.21 GHz, respectively, while all three switches (Sw1, Sw2, and

Sw3) are in the ON state having a gain of 1.85 dBi and 2.75 dBi respectively. The antenna operates in dual band mode (2.6 and 5.2 GHz) with a return loss of -45.8179 and -29.3527 dB, having a gain of 2.21 dBi and 3.46 dBi respectively, when the

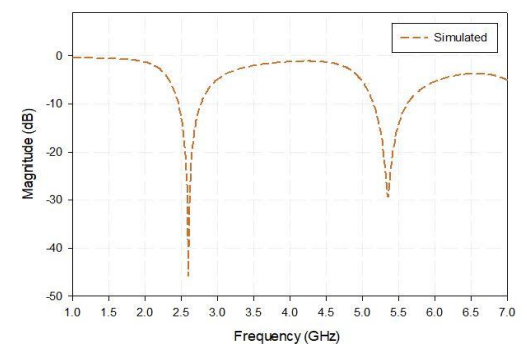
two switches (Sw1 and Sw2) are ON and Sw3 is OFF. The antenna operates in a single band mode at 3.5 GHz with a return loss of -24.3420, if one switch (Sw1) is switched ON and the other two switches (Sw2 and Sw3) are turned OFF with the gain of 3.57 dBi. The designed antenna operates in a single band mode at 5.4 GHz with a return loss of -17.1955 dB when all the switches are turned OFF having the gain of 4.42 dBi. Multiple processes and techniques of the antenna are accomplished using three lumped elements (RLC) switches, as indicated in Table 6.2. The lumped element switch was chosen because it can be simply modelled in Ansys HFSS as a $1\ \Omega$ and $1\text{M}\Omega$ resistor, respectively, to describe the switch-ON and switch-OFF states. Figure 6.3 depicts the simulated and measured reflection coefficients of the antenna.



(a)



(b)



(c)

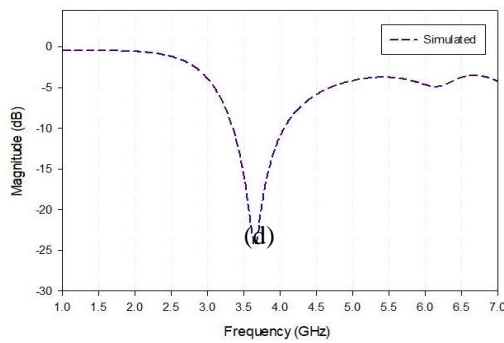


Figure 6.3. Simulated and Measured Reflection Coefficients of the operation states (a) Dual band (2.29 GHz and 4.21 GHz), (b) Single band (5.4 GHz), (c) Dual band (2.6 GHz and 5.2 GHz), (d) Single band (3.5 GHz).

PIN diodes (Skyworks SMP 1345-079LF) with low capacitance and strong result up to 6 GHz were specified for the experimental setup. When the diode is forward biased, it functions as a series resistor with a value of 1.5, whereas when reverse biased, it operates as a series capacitor with a value of 0.17 pF. It's important to remember that the constructed antenna's feeding line is totally separated from the DC path. Although capacitors can stop DC while allowing RF signals, and RF chokes can restrict RF while passing DC, an integration of the two issues should suffice. For RF choking, 125 nH inductors are required, and 470 pF capacitors are often used to short the RF signals released from the choking inductor. Two Alkaline AA batteries do provide biased voltage of 3V and the biased current of roughly 10 mA. An Agilent N5242A PNA-X Series Vector Network Analyzer is used to test the reconfigurable monopole antenna's reflection coefficient (S11). The VSWR of the designed antenna is less than 1.3 for all the frequency bands, which proves that the antenna is optimally matched. VSWR at 2.29, 4.21, 2.6, 5.2, 3.5, and 5.4 GHz is as given in Figure 6.4 and the Fabricated prototype is given in Figure 6.5.

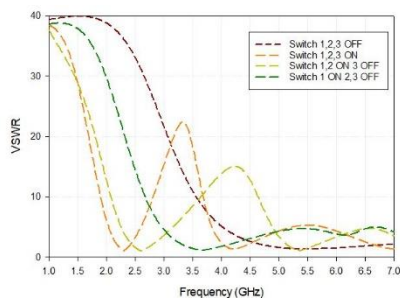


Figure 6.4. VSWR of the proposed antenna.

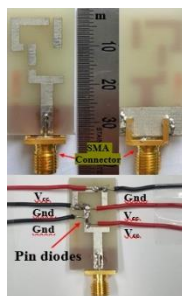


Figure 6.5. Fabricated Prototype.

An azimuth turntable is used to mount the manufactured antenna on the elevation. Because the antenna is linearly

polarized, the H- and E-plane radiation patterns are examined to get insight into the antenna's radiation characteristics in the two orthogonal planes. It's worthy to note that the designed hexa-band antenna radiates in an Omni direction and has dominating patterns in the horizontal H-plane throughout all six frequency bands. The antenna is designed in a single band mode with a peak gain of 3.26 dBi at 5.4 GHz by altering the modes of the switch. The suggested antenna operates in a dual band mode with peak gain values of 2.21 dBi and 3.46 dBi at 2.6 GHz and 5.2 GHz frequency bands, respectively, while SW1 and SW2 switches are ON and SW3 switch is OFF. The antenna operates in an only one resonant mode with a peak gain value of 2.38 dBi at 3.5 GHz when SW2 and SW3 are turned OFF and SW1 is turned ON. The designed antenna's determined H-plane exhibits an omnidirectional radiation pattern, whereas the E-plane has a substantially "figure of 8" form in all six resonant bands, as shown. The 3D far-field radiation patterns for the respective frequency bands are provided in Figure 6.6 for further understanding.

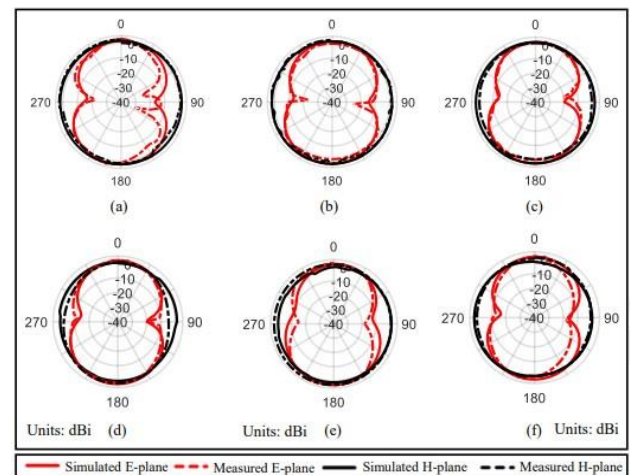


Figure 6.6. The simulated and measured radiation Pattern of antenna in E-plane (XOY) and H-plane (XOZ) at: (a) 2.29 GHz, (b) 4.21 GHz, (c) 2.6 GHz, (d) 5.2 GHz, (e) 3.5 GHz, (f) 5.4 GHz.

Figure 6.7 shows the calculated and measured H-plane and E-plane gain patterns for the following frequencies: 2.29 GHz, 4.21 GHz, 2.6 GHz, 5.2 GHz, 3.5 GHz, and 5.4 GHz. The antenna radiates in the far field region with peak gain values of every frequency are given below. Because of the matched feeding mechanism used throughout the design at the desired alignment, the proposed antenna radiates efficiently. The radiation efficiency of the designed antenna is 91.54%, 89.53 %,87.08%, 97.52%, 84.21% and 96.45% at 2.29 GHz, 4.21 GHz, 5.4 GHz, 2.6 GHz, 5.2 GHz and 3.5 GHz frequency bands respectively. The table following summarizes the entire performance of the proposed hexa-band antenna. The suggested hexa-band antenna is analyzed to the literature in the table below, which shows that the designed antenna is considerably smaller, has the most operating bands, has the highest gain, and provides the most bandwidth when related to the other works.

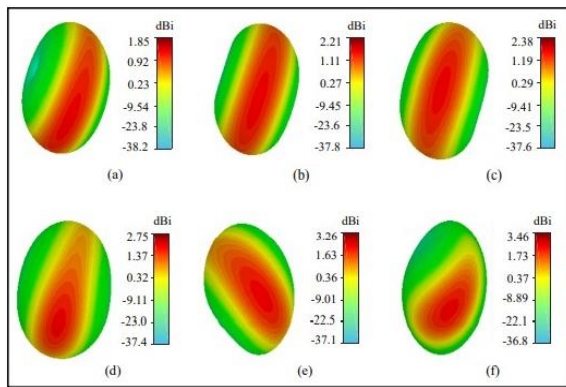


Figure 6.7. The 3D far-field gain pattern at: (a) 2.29 GHz. (b) 4.21 GHz. (c) 2.6 GHz. (d) 5.2 GHz. (e) 3.5 GHz. (f) 5.4 GHz.

3. CONCLUSIONS

In this work, a Novel hexa-band frequency reconfigurable monopole antenna has been designed and experimentally validated. The designed antenna was reconfigured to operate in two dual bands and two single band modes. When all the switches were in ON state, the proposed antenna operated in a dual band mode and when all the switches were in OFF state, the antenna performed in a single band mode. If two were in ON and one was in OFF state, it is operated in a dual band and when two switches were in OFF and one was in ON state, the antenna operated at a single resonant band. The outstanding efficiencies, satisfactory radiation patterns, acceptable gain, better impedance matching and directivity values were achieved for the different operating conditions of the proposed hexa-band antenna. The designed antenna has many advantages due to its characteristics such as light weight, compact size, low-cost, easy to fabricate and also simple in integration. The designed antenna can be intended for use in the satellite communications, military purposes and in modern communication devices such as laptops and tablets. Moreover, the measurement was conducted for the reflection coefficient and radiation patterns using PIN diodes in the fabricated prototype. The measured results of the proposed antenna were in a good agreement with the simulated results.

REFERENCES

- [1] Osman M N, Rahim M K A, Gardner P, Hamid M R, Yusoff M F M and Majid H A, "An electronically reconfigurable patch antenna design for polarization diversity with fixed resonant frequency", *Radio Eng.*, 24(1):45–53, (2015).
- [2] Saraswat R K and Kumar M, "A frequency band reconfigurable UWB antenna for high gain applications", *Prog Electromagn Res.*, 64:29–45, (2015).
- [3] Yeom I, Choi J, Kwoun S, Lee B and Jung C, "Analysis of RF front-end performance of reconfigurable antennas with RF switches in the far field", *Int J Antennas Propag.*, (2014).
- [4] Ullah S, Hayat S, Umar A, Ali U, Tahir F A and Flint J A, "Design, fabrication and measurement of triple band frequency reconfigurable antennas for portable wireless communications", *AEU-Int J Electron Commun.*, 81:236–242, (2017).
- [5] Shah I A, Hayat S, Khan I, Alam I, Ullah S and Afridi A, "A compact, tri-band and 9-shape reconfigurable antenna for WiFi, WiMAX and WLAN applications", *Int J Wirel Microw Technol.*, 5:45–53, (2017).
- [6] Anand S and Gloria J J, "RF MEMS based reconfigurable rectangular slotted self-similar antenna", *Circuits and Systems*, 7(06): 859, May 4, (2016).
- [7] Saleh A A and Abdullah A S, "A novel design of patch antenna loaded with complementary split-ring resonator and L-shape slot for (WiMAX/WLAN) applications", *Int J Wirel Microw Technol IJWMT*, 4(3):16–25, (2014).
- [8] Khan M F, Shah S A and Ullah S, "Dual-band frequency reconfigurable microstrip patch antenna on wearable substrate for Wi-Fi and Wi-MAX applications", *Technical Journal*, University of Engineering and Technology, Taxila, Pakistan, 22:35–40, (2017).
- [9] Hayat S, Shah I A, Khan I, Alam I, Ullah S and Basir A, "Design of tetra-band frequency reconfigurable antenna for portable wireless applications", *"Intelligent Systems Engineering (ICISE)*, IEEE, (pp. 10–13), Jan 15, (2015).
- [10] Hamid M R, Gardner P, Hall P S and Ghanem F, "Vivaldi antenna with integrated switchable band pass resonator", *IEEE transactions on antennas and propagation*, 59(11):4008–4015, (2017).
- [11] Iqbal A, Ullah S, Naeem U, Basir A and Ali U, "Design, fabrication and measurement of a compact, frequency reconfigurable, modified T-shape planar antenna for portable applications", *Journal of Electrical Engineering and Technology*, 12(4):1611–1618, (2017).
- [12] Ahyat E N, Kamarudin M R, Rahman T A, Jamlos M F, Hamid M R, Jamaluddin M H and Ramli N H, "Frequency and pattern reconfigurable dipole Yagi antenna", *Microwave and Optical Technology Letters*, 55(2):447–450, (2013).
- [13] Li Y and Li W, "A circular slot antenna with wide tunable and reconfigurable frequency rejection characteristic using capacitance loaded split-ring resonator for UWB applications", *Wireless personal communications*, 78(1):137–149, (2014).
- [14] Shah S A, Khan M F, Ullah S, Basir A, Ali U and Naeem U, "Design and measurement of planar monopole antennas for multi-band wireless applications", *IETE Journal of Research*, 63(2):194–204, (2017).
- [15] Ali T, Khaleeq M M and Biradar R C, "A multiband reconfigurable slot antenna for wireless applications", *AEU-International Journal of Electronics and Communications*, 84:273–280, (2018).
- [16] Ullah S, Ahmad S, Khan B A and Flint J A, "A multi-band switchable antenna for Wi-Fi, 3G Advanced, WiMAX, and WLAN wireless applications", *International Journal of Microwave and Wireless Technologies*, 1–7, (2018).
- [17] Sumit, "Reconfigurable fractal tree antenna for multifrequency applications using PIN diode", *International Journal of Engineering Research and Technology (IJERT)*, Vol. 3 Issue 4, April (2014).

[18] Mohan, Rayirathil K. Athira, and Kanagasabapathi G. Padmasine. "A Review on Materials and Reconfigurable Antenna Techniques for Wireless Communications: 5G and IoT Applications." *Progress in Electromagnetics Research B* 97 (2022).

[19] Mohan, Rayirathil K. Athira, and Kanagasabapathi G. Padmasine. "A Slotted Compact Four-Port Truncated Ground Structured MIMO Antenna for Sub-6 3.4 GHz 5G Application." *Progress in Electromagnetics Research C* 122 (2022).